Structure of the $N = Z = 28$ Closed Shell Studied by Monte Carlo Shell Model Calculation

Takaharu Otsuka,[1,2] Michio Honma,[3] and Takahiro Mizusaki[1]

[1]*Department of Physics, University of Tokyo, Hongo, Tokyo 113, Japan*
[2]*RIKEN, Hirosawa, Wako-shi, Saitama 351-01, Japan*
[3]*Center for Mathematical Sciences, University of Aizu, Tsuruga, Ikki-machi Aizu-Wakamatsu, Fukushima 965, Japan*
(Received 2 September 1997)

The closed shell structure at $N = Z = 28$ is studied by a large-scale shell model calculation by the quantum Monte Carlo diagonalization method. Latest crucial improvements of the method are described. The doubly closed shell probability of ^{56}Ni is shown to be only 49% in a full pf shell calculation, in contrast to the corresponding probability of ^{48}Ca which reaches 86%.
[S0031-9007(98)06895-1]

Quantum Monte Carlo approaches to many-body problems have been developed recently in various forms. For the nuclear shell model, the shell model Monte Carlo (SMMC) [1] and the quantum Monte Carlo diagonalization (QMCD) [2–4] methods have been proposed and developed so that they have practical applications. In this Letter we report the latest crucial improvements of the QMCD method and then discuss its application to the structure of ^{56}Ni. The nucleus ^{56}Ni is one of the unstable $N = Z$ nuclei. Its doubly magic structure has been expected [5], while the closed shell is evidently one of the key dominating structures of nuclei, which is of much general interest. Also, features of yrast states of ^{56}Ni are discussed up to 12^+, presenting intriguing irregularities.

We first briefly sketch the QMCD method [2–4]. We consider the imaginary time evolution operator $e^{-\beta H}$ for the Hamiltonian H, and divide β into N_t slices: $e^{-\beta H} = \prod_{n=1}^{N_t} e^{-\Delta\beta H}$, where $\Delta\beta = \beta/N_t$. By applying the Hubbard-Stratonovich (HS) transformation [6], we can express $e^{-\beta H}$ as the integration of an operator, $\prod_{n=1}^{N_t} e^{-\Delta\beta h(\vec{\sigma}_n)}$, where H is the shell model Hamiltonian consisting of single-particle energies and a two-body interaction, $h(\vec{\sigma})$ is a one-body operator, and the $\vec{\sigma}$ denotes a set of auxiliary fields, i.e., integral variables. The $h(\vec{\sigma})$ contains parameters determined by H and includes each component of $\vec{\sigma}$ linearly. In the QMCD method, we generate $\sigma \equiv \{\vec{\sigma}_1, \ldots, \vec{\sigma}_{N_t}\}$ stochastically and obtain many-body basis states of the form [2]

$$|\Phi(\sigma)\rangle \propto \prod_{n=1}^{N_t} e^{-\Delta\beta h(\vec{\sigma}_n)}|\Psi^{(0)}\rangle, \qquad (1)$$

where $|\Psi^{(0)}\rangle$ is an initial state. These states are called QMCD bases. The Hamiltonian is diagonalized within the Hilbert subspace spanned by the QMCD bases. Their number is called the QMCD basis dimension.

It is convenient to adopt QMCD bases in the form of Slater determinants: $|\Phi\rangle = \prod_{\alpha=1}^{N} a_\alpha^\dagger|-\rangle$, where N denotes the number of valence nucleons, $|-\rangle$ is an inert spherical core, and $a_\alpha^\dagger$ represents the nucleon creation operator for a canonical single-particle state α, which is

a linear combination of the spherical bases. Note that the form of a Slater determinant is kept in Eq. (1).

The formulation of the QMCD method is divided into three phases. In the first stage, i.e., phase I, the QMCD bases are generated according to Eq. (1) [2]. Phase I has been shown to be good for simple systems [2]. It was realized, however, that phase I is not efficient enough for handling realistic shell model systems [4].

We then introduced several improvements, moving to phase II [4], so as to enhance the efficiency of the QMCD calculations. Since, in practice, the number of manageable bases is finite, we should first select bases of higher importance. Thus, we rewrite $h(\vec{\sigma})$ so that the sampling of the bases is made around a mean-field solution, for instance, a Hartree-Fock (HF) local minimum.

The other improvement made concerned the restoration of symmetries [3,4]. The nucleus is an isolated system and conserves several symmetries. Their restoration is practically impossible in stochastic processes, except for extremely simple cases, as treated in [2], and one has to enforce the restoration. Rotational symmetry is restored by the J drive [4] and the M projection [3], where the angular momentum is represented by its magnitude J and z component M. The isospin is conserved properly [4].

Phase II means the combination of all of the above improvements and enabled us to perform various full one-major-shell calculations with realistic effective interactions [4]. Although decent solutions have then been obtained for most cases, it turned out that the calculation cannot be achieved with tractable QMCD dimensions in some cases. We, therefore, improve the method, resulting in phase III. We first recall the basis generation in phase II: The QMCD bases $|\Phi_1\rangle, |\Phi_2\rangle, \ldots, |\Phi_n\rangle$ are assumed to be already fixed. We then assume that, as the calculation proceeds, states are generated by Eq. (1), and $|\phi_1\rangle, |\phi_2\rangle, \ldots, |\Phi_k\rangle$ are adopted as bases, because they lower the energy sufficiently [2,4]. The eigenstate is then expanded as $|\psi\rangle \sim \sum_i c_i|\Phi_i\rangle + \sum_i d_i|\phi_i\rangle$, where the c's and d's are amplitudes. This is how phase II proceeds. It has been noted that the bases $|\phi_1\rangle, \ldots, |\Phi_k\rangle$ are usually quite redundant, and the value of k becomes too large in some cases, before a reasonable

convergence is achieved. This is partly because a basis $|\phi_i\rangle$ may have rather poor overlap with $|\psi\rangle$, and partly because $|\phi_i\rangle$ may contain components absent in $|\psi\rangle$ to be canceled by other bases.

This deficiency is inherent to the stochastic process, due to unavoidable fluctuations. Hence, we revised the basis-generation method. Again, suppose that the bases $|\Phi_1\rangle, \ldots, |\Phi_n\rangle$ are fixed already. One then generates the next basis. In the above discussion on phase II, it is $|\phi_1\rangle$. In phase III, for a candidate of the next basis $|\chi_1\rangle$, states $|\chi_2\rangle, \ldots, |\chi_l\rangle$ are generated by Eq. (1) in the vicinity of $|\chi_1\rangle$. We then calculate the energy eigenvalues with different sets of bases, $\{|\Phi_1\rangle, \ldots, |\Phi_n\rangle, |\chi_i\rangle\}$ by changing i from 1 to l, and find $|\chi_\alpha\rangle$ giving the lowest value. We repeat this process: bases $|\chi_2^{(1)}\rangle, \ldots, |\chi_{l'}^{(1)}\rangle$ are generated in the vicinity of $|\chi_\alpha\rangle$ ($\equiv |\chi_1^{(1)}\rangle$) similarly, and $|\chi_\beta^{(1)}\rangle$ giving the lowest energy is selected, etc. After reaching reasonable saturation, one ends up with a state $|\xi_1\rangle$, which should serve as the QMCD basis $|\Phi_{n+1}\rangle$. Compared to $|\phi_1\rangle$, $|\xi_1\rangle$ should be improved as a single basis in the sense that it contains more relevant components lowering the energy and less irrelevant components to be canceled by other bases. To be intuitive, these relevant components scattered in $|\phi_1\rangle$, $|\phi_2\rangle, \ldots$ are gathered to a good extent into $|\xi_1\rangle$. By proceeding with this quasivariational process, the bases $|\xi_1\rangle$, $|\xi_2\rangle, \ldots$ are obtained as $|\Phi_{n+1}\rangle$, $|\Phi_{n+2}\rangle, \ldots$, respectively, instead of $|\phi_1\rangle$, $|\phi_2\rangle, \ldots$. Naturally, the number of the above $|\xi\rangle$'s is much smaller than that of the above $|\phi\rangle$'s for the same accuracy. This means that the Hilbert space used for the Hamiltonian diagonalization can be greatly compressed. The usage of such compressed bases enables us to carry out some QMCD calculations which are otherwise practically infeasible.

For $|\chi_1\rangle$ created by Eq. (1) with σ_1, the other states $|\chi_i\rangle$'s ($i = 2, \ldots, l$) are generated, respectively, with $\sigma_1 + \delta\sigma_i$, by still using Eq. (1) but introducing certain shifts $\delta\sigma_i$'s. Each $\delta\sigma_i$ is a set of vectors with many components. Generally, individual components are shifted independently. Since the σ's can be considered to specify the path in the path integral interpretation of Eq. (1), the path is diffused in this revision, and the most favorable path is selected. This path diffusing method is easily incorporated into the calculation and turns out to be extremely useful. There are various flexibilities in the concrete manner of the path diffusing, for instance, how much the path is diffused. What is important is the basis selected. We have confirmed that the final results are insensitive to such details, if the calculation comes to reasonable saturation. The path diffusing is carried out already for the first basis.

The HS transformed imaginary-time evolution operator [see Eq. (4) of [2]] with Monte Carlo (MC) sampling is not used as the projection operator in the QMCD method. Instead, we utilize the property that it should produce states comprised mainly of dominant components

of low-lying eigenstates with larger relative probabilities or higher redundancies with different sets of the σ's, both of which yield larger net probabilities of the dominant components. On the other hand, it is unlikely that this MC sampling hits precisely one of the favorable states as the QMCD bases. In phase III, therefore, the σ's are first produced by the original MC sampling, but the candidate state is refined as stated above. Since only favorable states are then selected, one can compress the basis space. This compression process is one of the characteristic differences of the QMCD method from other quantum Monte Carlo approaches, where a much larger number of states in the form of Eq. (1) are taken so as to evaluate the effects of their proper superposition.

We now move on to the other major improvement, i.e., the restoration of the angular momentum, J. The J drive introduced in [4] is useful, but is sometimes unable to go beyond accuracy $\langle (J \cdot J) \rangle \sim 0.1$ for the 0^+ ground state in full pf-shell calculations. In order to remove uncertainties associated with this, all QMCD basis vectors are projected onto good J and M, when their matrix elements are calculated. The K-mixing amplitudes are evaluated, for instance, so as to minimize the energy when the basis is added. Thus, the uncertainty concerning angular momentum is completely removed in practice. Note that the rotation about the Euler axes is actually performed by numerical integration with sufficiently large numbers of mesh points.

The bases are varied and selected in the most natural way by monitoring the energy obtained from matrix elements projected onto good J and M, denoted as J-*compressed* bases. This process, however, requires a longer computation time. Instead, we can use the energy obtained by projecting onto only M (usually with $M = J$), resulting in M-*compressed* bases. The M-compressed bases are generated much faster, and yet appear to be quite good. We use them unless otherwise stated. When an M-compressed basis is fixed and added to the basis set, the Hamiltonian matrix is computed with the projection onto good J and M and is diagonalized. Isospin is treated exactly by utilizing the method in [1].

For a rotationally invariant Hamiltonian, energies are M degenerate. This degeneracy makes the calculation slower while it is removed by projecting onto M. Thus, M projection is crucial in basis generation.

The validity of phase III has been confirmed by comparing with the exact result for ^{48}Cr [7]. With the QMCD dimension 40, the ground-state energy has been reproduced within 130 keV. Excitation energies have been reproduced even better, e.g., within 30 keV up to 10^+.

We apply the QMCD shell model in phase III to an $N = Z$ nucleus, ^{56}Ni, where the $N = Z = 28$ closed shell structure has been expected due to the spin-orbit splitting [5]. Since this closed shell can be destroyed by mixing within the same major shell, the calculation with the full pf-shell configurations is crucial. Such calculations, however, have been limited to lighter

pf-shell nuclei. The QMCD calculation presented below is the first full pf-shell calculation for ^{56}Ni.

The single-particle energies and two-body interaction are those called FPD6 [8] and KB3 [9]. The FPD6 is an empirical two-body interaction adjusted for $A = 41$–49 nuclei [8]. The KB3 is based upon the G matrix in [10] with slight empirical improvement [9]. In both cases, the single-particle energies are obtained from experimental levels of nuclei around ^{40}Ca. We stress that both the FPD6 and KB3 interactions have been designed for full pf-shell calculations.

The KB3 has been shown to be quite good for pf-shell nuclei with Z, N up to ~ 26 [7,11]. On the other hand, the FPD6 has certain advantages for heavier nuclei, including ^{56}Ni, owing to a better effective gap between $f_{7/2}$ and the other pf-shell orbits, produced by a somewhat different monopole component [11,12]. On the other hand, these two interactions should have rather similar multipole components [13]. Therefore, the following discussions are only for the FPD6. Some results with the KB3 are also shown, as specifically mentioned.

Figure 1 shows energy levels of ^{56}Ni up to 12^+. One sees a good agreement between calculation and experiment [14]. Experimental yrast levels are well reproduced including intriguing irregularities. This agreement suggests the validity of the present calculation. For studying high-spin states, the method is improved by taking the cranked HF scheme, instead of the normal one, in the basis generation process, so as to increase high-spin components in the bases. Note that this change is only for the basis generation and the original Hamiltonian is diagonalized for calculating the energy eigenvalue.

We now turn to $E2$ transitions. Recently $B(E2; 0_1^+ \rightarrow 2_1^+) = 600 \pm 120 \ e^2 \text{fm}^4$ has been measured, which is rather large [15]. The FPD6 effective charges [8] produce a somewhat too large value, and the isoscalar charge is readjusted by multiplying by a factor of 0.9, result-

ing in $e_p = 1.23e$ and $e_n = 0.54e$. One then obtains $B(E2; 0_1^+ \rightarrow 2_1^+) = 610 \ e^2 \text{fm}^4$. The $B(E2)$'s are calculated also for the high-spin states with these charges, as shown in Fig. 1. Figure 1 also includes results obtained with KB3.
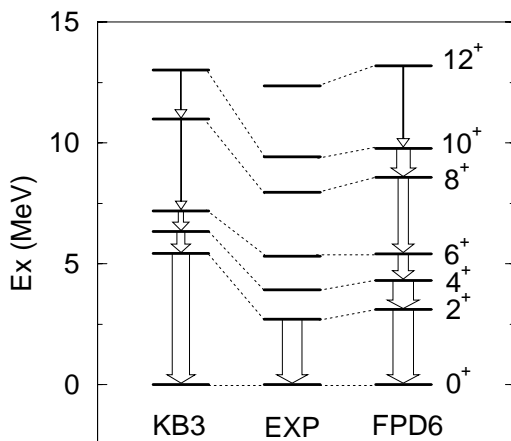
One of the salient advantages of the QMCD method over other quantum Monte Carlo approaches, including the SMMC, is its capability of direct analysis of the wave function. This is particularly important in the present case in clarifying the $N = Z = 28$ closed shell structure: We compute the probability of the $N = Z = 28$ closed shell component in the wave function of the ^{56}Ni ground state. The result is only 49%. This is rather small compared to what would be expected for a closed shell nucleus. The occupation probability of $f_{7/2}$ is 0.91 for the ground state. This means that, in the nondoubly magic part of the wave function, about three nucleons are excited from $f_{7/2}$ on the average. Thus, if a truncated shell model calculation were attempted, at least $6p6h$ excitations from $f_{7/2}$ should be included. The difference in the nucleon occupation number in $f_{7/2}$ is 1.6 between the ground and first 2^+ states, denying a simple $1p1h$ excitation picture.

We now discuss the structure of ^{48}Ca for comparison [8]. The wave function of the ^{48}Ca ground state contains the $N = 28$ and $Z = 20$ closed shell component with 86% probability. This is much larger than the corresponding value for ^{56}Ni. Thus, a sizable breaking of the $N = Z = 28$ doubly magic is seen in ^{56}Ni, especially compared to ^{48}Ca. If the $N = Z = 28$ shell of ^{56}Ni were broken by the same mechanism as the $N = 28$ shell of ^{48}Ca, the closed shell probability of ^{56}Ni would be given by the square of the corresponding value of ^{48}Ca: $(0.86)^2 = 0.74$. Clearly, the actual value, 0.49, is much smaller. This is because the $N = Z = 28$ shell of ^{56}Ni is broken largely due to interactions between a valence proton and a valence neutron, particularly terms with a quadrupole nature. This seems to be a consequence of strong proton-neutron correlations characterizing $N = Z$ nuclei, where the proton-neutron pairing may arise [16]. On the other hand, the neutron-neutron pairing should be the major cause of breaking the $N = 28$ shell in ^{48}Ca.

Figure 2 shows, as functions of the QMCD dimension, the 2_1^+, 6_1^+, and 10_1^+ levels. The angular momentum is restored in phase II as the QMCD dimension increases and converges as the energy does [4]. In phase III, each basis is projected onto good J and M, and the change is entirely due to the dynamical structure. Figure 2 indicates that excitation energies vary for small QMCD dimensions but become quite stable as the dimension becomes large enough (~ 20). Two lines for a given spin/parity mean results of two different calculations. The 4_1^+, 8_1^+, and 12_1^+ levels show similar trends.

We now compare energy levels of $J = 2 \sim 8$, obtained by the M-compressed bases, to those by the J-compressed bases. The differences are found to be rather small: $0.05 \sim 1\%$. Thus, the excitation energies can be

FIG. 1. Experimental (EXP) yrast levels of ^{56}Ni compared with QMCD results with FPD6 and KB3 Hamiltonians. The $B(E2; (L + 2)_1^+ \rightarrow L_1^+)$ value is indicated by the width of the arrow, which is so that the experimental $B(E2; 2_1^+ \rightarrow 0_1^+)$ value takes its mean value, i.e., $120 \ e^2 \text{fm}^4$ [15].
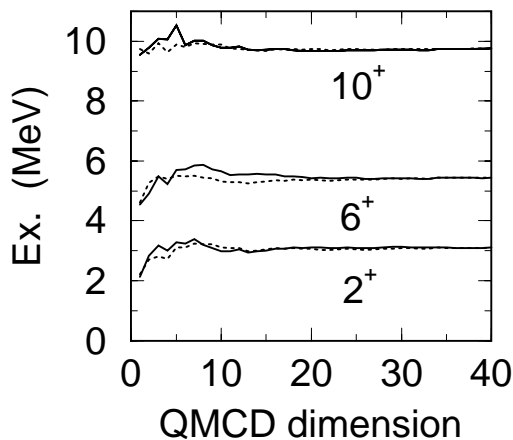
FIG. 2. Excitation energies as functions of QMCD dimensions. Solid and dotted lines correspond to two independent calculations.

evaluated to a good approximation with the M-compressed bases. The differences are slightly larger for $B(E2)$ values, because they are more sensitive to details of the wave functions. The $B(E2)$ values in Fig. 1 are calculated with the above J-compressed bases for the states below $J = 8$, for the sake of higher precision.

The ground-state energy becomes -203.100 MeV in a calculation with 30 J-compressed bases. This value is about 5.5 MeV below the HF energy. Although the ground-state energy still goes lower at this dimension, its gradient is rather small. The $M = 0$ Hilbert space has a dimension of $\sim 1.1 \times 10^9$ for ^{56}Ni in the full pf shell, whereas the dimension decreases to $\sim 25 \times 10^6$ in the truncation up to $6p6h$ excitations from the $f_{7/2}$ closed shell. In this truncation, the ground-state energy has been computed as -203.063 MeV by conventional methods [17,18]. In the QMCD, although the ground-state energy can be evaluated to a good extent, its exact value may not be reached, in general, because of fewer dimensions. On the other hand, certain physical quantities such as excitation energies show (near) convergence, as functions of the QMCD dimension. For instance, the 2_1^+ state exhibits this feature in Fig. 2. In the above $6p6h$ calculation, the 2_1^+ level remains ~ 0.4 MeV higher than this.

The $E2$ sum rule is 730 e^2 fm^4, $\sim 85\%$ of which is exhausted by the 2_1^+ state. The fact that the KB3 is too stiff for ^{56}Ni [11,19] can be confirmed by Fig. 1, where the 2_1^+ level of KB3 appears ~ 3 MeV above the experimental one. The $B(E2)$ values are shown in Fig. 1 also for the KB3 with effective charges $e_p = 1.5e$ and $e_n = 0.5e$ used in [7]. The $E2$ sum rule is 515 ± 40 e^2 fm^4 in the SMMC using the KB3 with $e_p = 1.35e$ and $e_n = 0.35e$ [19], in agreement with the QMCD value, 540 e^2 fm^4.

We will briefly discuss the results obtained by assuming an $N = Z = 28$ closed shell. If we assume that the 2_1^+ state is comprised of a $1p$-$1h$ excitation from the $N = Z = 28$ shell, its excitation energy becomes 4.2 (6.1) MeV for the FPD6 (KB3) interaction. This is significantly higher than the result of the full calculation, particularly for FPD6. Likewise, the $B(E2)$ sum rule becomes about half of the above value.

In summary, we have presented the latest major and crucial revision of the QMCD formulation. This revision, i.e., phase III, is characterized by the compression of the basis space and the precise treatment of the angular momentum. Thus, in the QMCD calculation, favorable bases are generated based upon their contribution to the energy eigenvalue, and quite naturally some of such bases or their seeds can be taken from mean-field solutions. The lowest levels of ^{56}Ni are then well described with the FPD6 interaction. It has been shown that the doubly closed shell structure is substantially broken in ^{56}Ni, in contrast to ^{48}Ca. The irregular level structure of higher-spin yrast states of ^{56}Ni is also reproduced, thus ensuring the validity of the present conclusion. In view of this study, the doubly closed shell structure of ^{100}Sn can be questioned and is becoming a more intriguing issue.

[1] S. E. Koonin, D. J. Dean, and K. Langanke, Phys. Rep. **278**, 1 (1997), and references therein.
[2] M. Honma, T. Mizusaki, and T. Otsuka, Phys. Rev. Lett. **75**, 1284 (1995).
[3] T. Mizusaki, M. Honma, and T. Otsuka, Phys. Rev. C **53**, 2786 (1996).
[4] M. Honma, T. Mizusaki, and T. Otsuka, Phys. Rev. Lett. **77**, 3315 (1996).
[5] See, for instance, A. Bohr and B. R. Mottelson, *Nuclear Structure* (Benjamin, New York, 1969), Vol. 1.
[6] J. Hubbard, Phys. Lett. **3**, 77 (1959); R. D. Stratonovich, Dokl. Akad. Nauk SSSR **115**, 1907 (1957) [Sov. Phys. Dokl. **2**, 416 (1958)].
[7] E. Caurier *et al.,* Phys. Rev. C **50**, 225 (1994).
[8] W. A. Richter *et al.,* Nucl. Phys. **A523**, 325 (1991).
[9] A. Poves and A. P. Zuker, Phys. Rep. **70**, 235 (1981).
[10] T. T. S. Kuo and G. E. Brown, Nucl. Phys. **A114**, 241 (1968).
[11] E. Caurier *et al.,* Phys. Rev. C **52**, 1736 (1995); G. Martinez-Pinedo *et al.,* Phys. Rev. C **55**, 187 (1997).
[12] W. E. Ormand and B. A. Brown, Phys. Rev. C **52**, 2455 (1995).
[13] M. Dufour and A. P. Zuker, Phys. Rev. C **54**, 1641 (1996).
[14] *Table of Isotopes,* edited by R. B. Firestone *et al.* (Wiley, New York, 1996); D. Rudolph *et al.* (private communication).
[15] G. Kraus *et al.,* Phys. Rev. Lett. **73**, 1773 (1994).
[16] J. Engel *et al.,* Phys. Lett. B **389**, 211 (1996).
[17] E. Caurier and A. Poves (private communication).
[18] T. Sebe *et al.* (private communication).
[19] K. Langanke *et al.,* Phys. Rev. C **52**, 718 (1995).